THE JOURNAL OF BIOLOGICAL CHEMISTRY
Vol. 276, No. 40, Issue of October 5, pp. 37482–37490, 2001
Printed in U.S.A.

Residues at the Active Site of the Esterase 2 from *Alicyclobacillus acidocaldarius* Involved in Substrate Specificity and Catalytic Activity at High Temperature*

Received for publication, April 5, 2001, and in revised form, July 5, 2001
Published, JBC Papers in Press, July 10, 2001, DOI 10.1074/jbc.M103017200

Giuseppe Manco‡, Luigi Mandrich, and Mosè Rossi

From the Institute of Protein Biochemistry and Enzymology, Consiglio Nazionale delle Ricerche, via G. Marconi 10, Naples 80125, Italy

The recently solved three-dimensional structure of the thermophilic esterase 2 from *Alicyclobacillus acidocaldarius* allowed us to have a snapshot of an enzyme-sulfonate complex, which mimics the second stage of the catalytic reaction, namely the covalent acyl-enzyme intermediate. The aim of this work was to design, by structure-aided analysis and to generate by site-directed and saturation mutagenesis, EST2 variants with changed substrate specificity in the direction of preference for monoacylesters whose acyl-chain length is greater than eight carbon atoms. Positions 211 and 215 of the polypeptide chain were chosen to introduce mutations. Among five variants with single and double amino acid substitutions, three were obtained, M211S, R215L, and M211S/R215L, that changed the catalytic efficiency profile in the desired direction. Kinetic characterization of mutants and wild type showed that this change was achieved by an increase in k_{cat} and a decrease in K_m values with respect to the parental enzyme. The M211S/R215L specificity constant for *p*-nitrophenyl decanoate substrate was 6-fold higher than the wild type. However, variants M211T, M211S, and M211V showed strikingly increased activity as well as maximal activity with monoacylesters with four carbon atoms in the acyl chain, compared with the wild type. In the case of mutant M211T, the k_{cat} for *p*-nitrophenyl butanoate was 2.4-fold higher. Overall, depending on the variant and on the substrate, we observed improved catalytic activity at 70 °C with respect to the wild type, which was a somewhat unexpected result for an enzyme with already high k_{cat} values at high temperature. In addition, variants with altered specificity toward the acyl-chain length were obtained. The results were interpreted in the context of the EST2 three-dimensional structure and a proposed catalytic mechanism in which k_{cat}, *e.g.* the limiting step of the reaction, was dependent on the acyl chain length of the ester substrate.

Esterases, lipases, and cholinesterases belong to a superfamily of phylogenetically related proteins with representatives in the domains of Eukarya, Bacteria, and Archaea (1–6). These proteins are divided into three groups based on their sequence identity: the C group, which includes cholinesterases and fungal lipases, the L group, which includes lipoprotein lipases and bacterial lipases, and the H group, named after the hormone-sensitive lipase (HSL)[1] discovered by Holm *et al.* (7), which comprises proteins showing sequence similarity with HSL. Some years ago, Hemilä *et al.* (2) reported a new gene from the thermophilic strain *Alicyclobacillus acidocaldarius*, encoding a protein of unknown function with sequence similarity to the catalytic domain of mammalian HSL. The identification of other related sequences allowed the definition of the H group.

We focused on this thermostable member of the family, which we first identified in a crude extract of *A. acidocaldarius* and named esterase 2 (EST2) (5). To study its structure-function relationships in detail, we overexpressed the functional protein in *Escherichia coli* and purified and characterized the recombinant enzyme, which was demonstrated to be a monomeric B-type carboxylesterase of about 34 kDa. The enzyme displays an optimal temperature at 70 °C and remarkable temperature stability with a half-life of 3 h at 75 °C. Maximal activity was observed with para-nitrophenyl (*p*NP) esters with acyl chains of six to eight carbon atoms (8). Residues belonging to the catalytic triad were identified as Ser-155, Asp-252, and His-282 (9). The information concerning the thermostability within the esterase/lipase family was also interesting (10). To further address this point, we cloned, overexpressed, characterized, and constructed a model for the related esterase from the archaeon *Archaeoglobus fulgidus* (6, 11).

Recently, Wei *et al.* (12) solved the structure of brefeldin A esterase from the strain *Bacillus subtilis*, which turned out to belong to the H group. This was the first member of the group to be structurally characterized. More recently, we reported (13) the crystal structure of EST2 complexed with a substrate analogue solved by multiple wavelength anomalous diffraction on a seleno-methionine derivative, at 2.6-Å resolution. The two structures revealed a common topological α/β-hydrolase fold, which is well known among lipases (14–16). This fold is characterized by a central, mixed β-sheet, flanked by helical connections. Moreover, the catalytic center contains a triad of amino acids (SH(D/E)) reminiscent of serine proteinases, which is responsible for the nucleophilic attack on the carbonyl carbon of the scissile ester bond. However, the two structures differ from the canonical α/β-hydrolase fold because of the lack of the helix αD and the presence of a cap that covers and protects the active site (12, 13); therefore, the H group may well represent a new family in contrast with a classification previously proposed (17). Actually, in the ESTHER classification (18), the two structures define the HSL family, which, to date, comprises more than 64 members.

* This work was supported by a grant from Recordati Industria Chimica e Farmaceutica Spa. The costs of publication of this article were defrayed in part by the payment of page charges. This article must therefore be hereby marked "*advertisement*" in accordance with 18 U.S.C. Section 1734 solely to indicate this fact.

‡ To whom correspondence should be addressed: Tel.: 39-81-725-7316; Fax: 39-81-725-7240; E-mail: manco@dafne.ibpe.na.cnr.it.

[1] The abbreviations used are: HSL, hormone-sensitive lipase; EST2, esterase 2; *p*NP, *p*-nitrophenyl; CD, circular dichroism; IPTG, isopropyl-β-D-thiogalactoside; PAGE, polyacrylamide gel electrophoresis.

Structural investigations on EST2 were undertaken to study its structure-function relationships in detail (13, 19, 20). Furthermore, esterases are enzymes of considerable industrial potential. According to a classical definition, esterases are lipolytic enzymes that, unlike lipases, hydrolyze soluble fatty acid esters without any interfacial activation (21, 22). The resistance to denaturation of thermophilic enzymes coupled with their ability to hydrolyze substrates that are insoluble at normal temperatures, makes thermostable lipases/esterases an attractive alternative to mesophilic enzymes (23). Although a few lipases have been so far reported from thermophilic sources (24–26), detailed characterizations have still not been performed.

The aim of this work was to obtain, through a combination of site-directed and saturation mutagenesis, variants of the thermophilic esterase with altered specificity, and in particular, better specificity against esters whose acyl chains were larger than eight carbon atoms. For the rational design of specific mutations, we took advantage of the availability of the EST2 structure complexed with a HEPES molecule, covalently bound to the active site Ser155. Although some variants were obtained with changes in the desired direction, the most striking result was the enhanced steady-state activity, depending on mutation and on substrate, of all the variants at 70 °C.

EXPERIMENTAL PROCEDURES

Materials—*p*-Nitrophenyl (*p*NP) esters, Fast Blue RR, β-naphthyl acetate, and β-naphthyl laurate were purchased from Sigma Chemical Co. (St. Louis, MO).

Strains and Plasmids—*E. coli* Top 10 (Invitrogen, Carlsbad, CA) was used as host for cloning whereas *E. coli* BL21(DE3) harbored the recombinant plasmids for gene expression. The expression vector utilized (pT7-SCII-AG) was prepared starting from vector pT7-SCII-MG1 (8). The est2 gene was amplified by using the pT7-SCII-MG1 vector, as template, recombinant *Taq* DNA polymerase, and oligonucleotides est5′ (5′-GGCGACCCATATGCCGCTCGATCCC-3′) and est3′ (5′-GCGCGAAGGGAAGATCCGCGCGTGTTCG-3′) as forward and reverse primers, respectively, in a 30-cycle polymerase chain reaction (1 min at 92 °C, 1 min at 55 °C, and 1 min at 72 °C). The amplification primer est5′ was designed to introduce a *Nde*I restriction site (underlined) upstream from the initiation site, whereas est3′ was located downstream from the stop codon of EST2 and from a *Sma*I restriction site located outside the coding region. The PCR product, eluted from an agarose gel and digested with *Nde*I and *Sma*I, was ligated into the *Nde*I-*Sma*I-linearized expression vector pT7-SCII to create the pT7-SCII-AG construct. The cloned fragment was completely sequenced on both strands using the T7 DNA polymerase sequencing kit (Amersham Pharmacia Biotech, Uppsala, Sweden) to verify that only desired mutations were introduced during amplification. In this way, the est2 gene was expressed under the direct control of the IPTG inducible promoter of the ϕ10 gene (27).

Mutagenesis, Cloning, and Overexpression—Standard molecular cloning techniques were utilized (28). The site-directed mutants presented in this study were prepared by the overlap extension method (29) with the polymerase chain reaction. The plasmid pT7-SCII-AG (this paper), a derivative of PT7-SCII-MG1 (8) was used as the template for amplification reactions carried out with the Expand high fidelity PCR system (Roche Molecular Biochemicals), using two end primers and two complementary mutagenic primers for each site-specific mutation. The sequences of the oligonucleotides used were as follows (mismatch sites for site-directed mutagenesis are in boldface): M211T (+), 5′-CCTGACCGGCGGCATGACGCTCTGGTTCCGGG-3′; M211T(−), 5′-CCCGGAACCAGAGCGTCATGCCGCCGGTCAGG-3′; R215L(+), 5′-GCTCTGGTTCCTGGATCAATACTTGAA-3′; R215L(−), 5′-TGTTCAAGTATTGATCCAGGAACCAGA-3′; the oligonucleotides used for the saturation mutagenesis were as follows: M211(+), 5′-CCTGACCGGCGGCATG(atgc)(atgc)(gc)CTCTGGTT-3′; M211(−), 5′-GGAACCAGAG(gc)(atgc)(atgc)CATGCCGCCGGTCA-3′. The two external oligonucleotides were: Ser(+), 5′-TCGGCGGAGACGGCGCCGGAGGGAA-3′; Cter(−), 5′-TTGGATCCGCCTTTTGGTCAGG-3′. Each amplification reaction was performed with 30 cycles of 94 °C for 1 min, 55 °C for 1 min, and 72 °C for 1 min. The final amplified products were cut appropriately with restriction enzymes, purified with an agarose gel-extraction kit (Quiaex II, M-Medical), ligated into pT77-SCII-AG or pT77-SCII-AGM215L, and linearized with the same restriction enzymes. The cloned DNA fragments were entirely sequenced to confirm the presence of the mutation(s) and to rule out the possibility that replication errors were introduced during amplification.

The ligation mixtures were used to transform *E. coli* Top 10. In the case of site-directed mutants, selected colonies were grown for plasmidic DNA preparation and mutations were confirmed by DNA sequencing. After IPTG-induced overexpression into *E. coli* BL21(DE3) cells, partially purified enzymes were assayed with esters of different acyl chain length (from 4 to 16). As regarding the saturation mutagenesis approach, a rapid screening on nitrocellulose filters was devised to select variants with interesting phenotypes. Briefly, the colonies obtained from plasmid transformation in *E. coli* Top 10 were replicated on two nitrocellulose filters and tested for esterase activity on β-naphthyl acetate or β-naphthyl laurate. The filters were subjected to three cycles of freezing and thawing to obtain cell disruption. Released proteins were fixed by 10-min incubation at 70 °C, and then filters were incubated in a solution (100 ml) of 100 mM Tris-HCl, pH 7.5, containing 5 mg of β-naphthyl acetate or β-naphthyl laurate (dissolved in 0.5 ml of methanol) and 25 mg of Fast Blue RR at room temperature. After 10–15 min of incubation, the reactions were stopped by rinsing with tap water. The activity toward β-naphthyl acetate was adopted initially as control of enzyme expression, whereas activity toward β-naphthyl laurate was employed to identify mutants with altered specificity. Successively, screening with β-naphthyl acetate was used to select mutants with altered specificity toward esters with shorter acyl chains. The changed selectivity was further controlled by spectrophotometric standard assay at 70 °C. DNA sequencing of extracted DNA allowed to identify the mutations. As a result, the mutants M211V, M211S, and M211S/R215L were obtained.

E. coli BL21(DE3) cells were transformed with the constructs and cultured at a large scale in 2 liters of Luria-Bertani (LB) medium supplemented with 100 μg of ampicillin. Cells were induced with 1 mM isopropyl-thiogalactopyranoside (IPTG) for 3 h at a cell density corresponding to an optical density of 1 $A_{600\ nm}$. Thereafter, cells were harvested by centrifugation (13,200 × *g*, 4 °C, 10 min), washed with 25 mM Tris-HCl buffer (pH 8.5)/2.5 mM $MgCl_2$/0.5 mM EDTA and stored at −20 °C.

Purification of the recombinant enzymes was performed as previously described for the wild type (8).

Enzyme Assays—The time course of the esterase-catalyzed hydrolysis of *p*NP esters was followed by monitoring of *p*-nitrophenoxide production at 405 nm, in 1-cm path-length cells with a DU 600 spectrophotometer (Beckman, Fullerton, CA). Initial rates were calculated by linear least-squares analysis of time courses comprising less than 10% of the total turnover.

Assays were performed at 70 °C in mixtures of 40 mM Na_2HPO_4/NaH_2PO_4/0.09% (w/v) gum arabic/7.5% propan-2-ol (pH 7.1) containing *p*NP esters at different concentrations. Stock solutions of *p*NP esters were prepared by dissolving substrates in pure propan-2-ol. Protein concentration was determined spectrophotometrically using an extinction coefficient of 43,300 $M^{-1}\ cm^{-1}$ at 278 nm.

Kinetic Measurements—Initial velocity *versus* substrate concentration data were fitted to the Lineweaver-Burk transformation of the Michaelis-Menten equation, by weighted linear least-squares analysis with a personal computer and the GRAFIT program (30). Assays were done in duplicate or triplicate, and results for kinetic data were mean of two independent experiments.

The inhibition by HEPES (sodium salt) and by propan-2-ol was evaluated by assaying EST2 activity in the standard assay in the presence of three different inhibitor's concentrations (0.2, 0.4, and 0.8 M for HEPES; 0.39, 0.65, and 0.89 M for propan-2-ol) and different concentrations of *p*NP-hexanoate (range 12.5–300 μM).

Electrophoreses—Electrophoretic runs were performed with a Bio-Rad Mini-Protean II cell unit, at room temperature. 12.5% SDS-PAGE was performed essentially as described by Laemmli (31). Gels were stained with Coomassie Brilliant Blue G-250. Molecular mass markers (Prestained SDS-PAGE Standard Broad Range, Bio-Rad) were: myosin (205 kDa), β-galactosidase (120 kDa), bovine serum albumin (84 kDa), ovalbumin (52 kDa), carbonic anhydrase (36 kDa), soybean trypsin inhibitor (30 kDa), lysozyme (22 kDa), and aprotinin (7.4 kDa).

Circular Dichroism (CD)—Far-UV (190–250 nm) CD measurements were performed in a spectropolarimeter model J-710 (Jasco, Tokyo, Japan) at 50 °C under nitrogen flow. A cuvette (Helma, Jamaica, NY) of 0.1 cm path-length was used. Photomultiplier absorption did not exceed 600 V in the spectral region measured. A spectral acquisition spacing of 0.2 nm (1.0-nm bandwidth) was used. Each spectrum was averaged five times and smoothed with Spectropolarimeter System Software version 1.00 (Jasco). Protein concentration of the samples was 0.10 mg/ml in 40

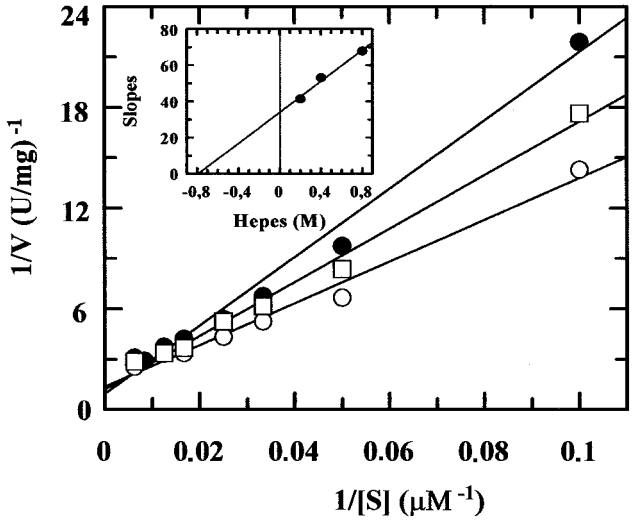

FIG. 1. **HEPES inhibition of wild type EST2.** Shown is the Lineweaver-Burk plot of EST2 activity measured in the concentration range 10–160 μM of *p*NP-hexanoate in the presence of 0.2 M (○), 0.4 M (□), and 0.8 M (●) HEPES, at 70 °C. In the *inset*, the slopes of the three lines were replotted against the inhibitor concentrations.

mM Na_2HPO_4/NaH_2PO_4, pH 7.1. To compare the thermal stability of wild type and mutant enzymes, spectral acquisition were achieved in the temperature range of 50–95 °C at 5 °C spacing. Moreover, the ellipticity readings at $\lambda = 222$ or $\lambda = 290$ nm were continuously monitored as the temperature was raised at 1 °C *per* min. The comparison was based on the midpoint measurements through the first derivative transformation of the denaturation curves, which appeared sigmoidal.

Near-UV (250–320 nm) CD measurements were performed at 40 °C with a 1-cm path-length cuvette (Starna Brand, Essex, UK). Protein concentration of the samples was 0.3 mg/ml in 40 mM Na_2HPO_4/NaH_2PO_4, pH 7.1.

Structure Analysis—The visualization of EST2 structure (PDB file: 1EVQ; Protein Data Bank, Rutgers University, Upton, NY), the molecular surface analysis, and the energy minimization to evaluate residues substitution were carried out with the Swiss PDB viewer program (Glaxo Wellcome Experimental Research).

RESULTS

HEPES Is a Competitive Inhibitor of EST2—The recently solved three-dimensional structure of the *A. acidocaldarius* EST2 revealed the fortuitous formation of a covalent adduct of the active site Ser-155 with a HEPES molecule (13). Although sulfonic esters, such as phenylmethylsulfonyl fluoride, are known to be irreversible inhibitors of the enzyme (8), the above finding was unexpected, because HEPES is a sulfonic acid and therefore the mechanistic explanation for the adduct formation remained elusive. To address this point, investigations were carried out to verify whether or not HEPES (sodium salt) may really be an EST2 inhibitor and thus whether the enzyme-HEPES complex is actually an example of a mimic of the second tetrahedral intermediate, corresponding to the de-acylation step of the catalytic reaction. At saturating concentrations of substrate *p*NP-hexanoate, high concentrations of HEPES (up to 1 M) did not affect the EST2 activity. Moreover, prolonged incubations of EST2 with HEPES (up to 12 h) had no effect on its catalytic activity (data not shown). Fig. 1 reports the Lineweaver-Burk plots of EST2 activity at three different HEPES concentrations. In the insert, a re-plot of the slope of each line against the respective inhibitor concentration is shown. From this analysis it turned out that HEPES is a competitive inhibitor of the enzyme with a calculate K_I of 0.78 M.

Because the enzyme is able to catalyze the reverse reaction of esterification in organic solvents (8), we could infer that the finding in the crystals of a covalent adduct with HEPES was likely to be due to the particular conditions of "low water activity" that the protein requires to crystallize. In these conditions, the reverse reaction was favored, and therefore, a stable HEPES-enzyme complex could be formed. In this way, the HEPES molecule should be regarded as a substrate analogue, which was trapped as an acyl-enzyme intermediate on the synthetic catalytic route. Thus, what we are looking at is the first half of the reverse synthetic reaction, more than the second half of the hydrolytic reaction, even though it is predictable that the molecular recognition mechanisms of the acyl moiety are the same in both cases.

Strategy for Protein Engineering—Fig. 2 schematically shows the protein-ligand interactions with the sulfur atom covalently bound to Ser-155 and its piperazine ethane moiety fitting into a long hydrophobic tunnel closed at the end mostly by the side chains of Met-211 and Arg-215. Detailed analysis of the solvent-accessible surface of the EST2 structure revealed the presence of two buried cavities, marked a and b, of 45 and 60 $Å^3$ respectively, nearby the active site (Fig. 2*B*). These two cavities are constellated with polar and charged residues to which water molecules are also hydrogen-bonded (Fig. 2*C*). In particular, cavity B of 60 $Å^3$, located nearby the acyl binding pocket, is the largest of the 16 cavities found in the EST2 structure, and it is surrounded by the following residues: Trp-85, Asn-159, Ser-185, Gly-187, Tyr-188, Met-211, Phe-214, Arg-215, Phe-230, Ser-231, Leu-254, and Val-257. Two water molecules, 20 and 57, are located inside the buried cavity and form a network of hydrogen bonds with the surrounding residues. In particular, Arg-215 forms hydrogen bonds through the NH_2 of its guanidinium group to water molecules 20, 38, and 57; moreover, another hydrogen bond is formed through NE of its side chain with water 38 that, along with 51, forms a second pair of water molecules involved in a network of hydrogen bonds with surrounding residues. Among these residues, Tyr-188 appears again. In contrast, Met-211 is not involved in hydrogen bonds, but its side chain participates in closing the hydrophobic tunnel at the bottom. We reasoned that a reduction in the steric hindrance afforded by the side chains of Met-211 and Arg-215 and eventually their substitution with residues that increase local hydrophobicity, could allow for a better binding of an ester with longer acyl chain.

A visual inspection of a structural alignment in the H group among EST2, the brefeldin A esterase, the *A. fulgidus* esterase, the *Moraxella TA144* lipase, the *E. coli* esterase, and the *human* hormone-sensitive lipase (13) indicated that the two lipases of the H group held the charged residue glutamate and the small residue glycine, respectively, in place of Met-211. Both the hydrophobic residue leucine and the shortest residue methionine were observed in place of Arg-215 in the *Moraxella TA144* lipase and *human* hormone-sensitive lipase, respectively. We decided to mutagenize residues Arg-215 and Met-211 to leucine and threonine, respectively, because lipases are more specific for esters with longer acyl chains.

Site-directed Mutagenesis, Saturation Mutagenesis, and Screening—The mutagenesis strategy adopted was to introduce first leucine at position 215 and threonine at position 211, by site-directed mutagenesis, and then to change the second site by saturation mutagenesis, if either of the two former substitutions was found to give the desired effect. To this end, we prepared the expression vector pT7SCII-AG, as described under "Experimental Procedures," which contains the *est2* gene under the direct control of the IPTG-inducible promoter of the ϕ10 gene (29). The availability of this clone yielded an easier way to handle the gene and to express the protein, which in the previously described expression system (8) was produced under the control of its own promoter.

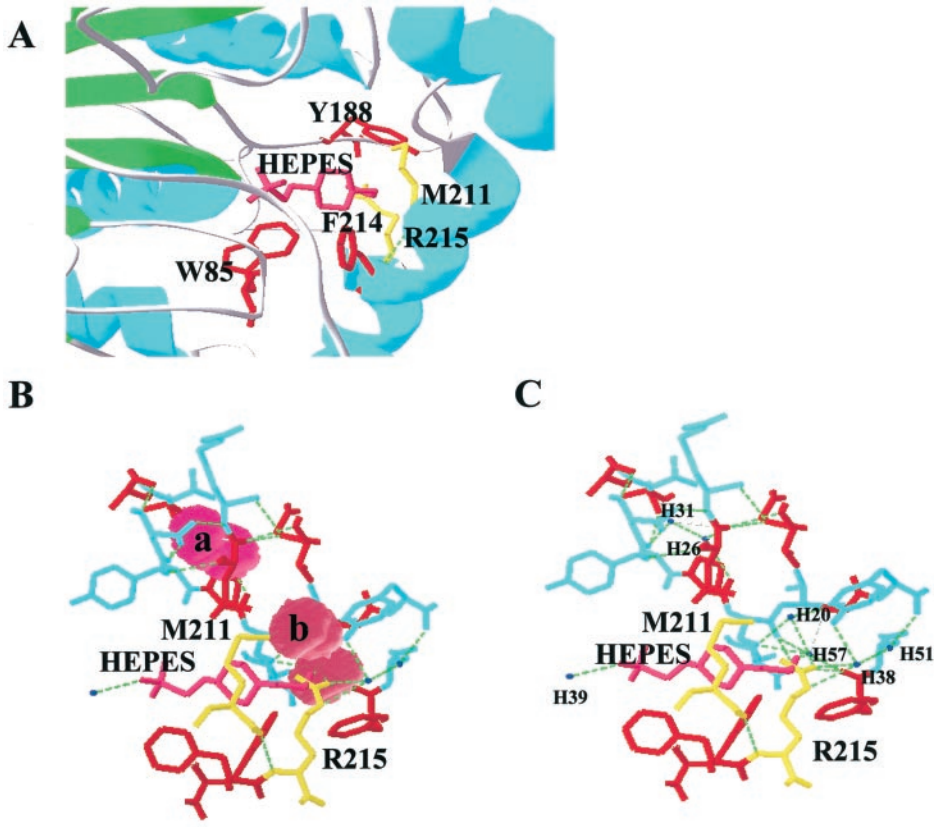

FIG. 2. **View of the EST2 active site with the HEPES molecule.** Shown in *A* are the interactions of the HEPES molecule (in *pink*) with surrounding residues and, in particular, with Arg-215 and Met-211 (in *yellow*), which close the acyl binding pocket. Also shown (in *red*) are the aromatic residues near the acyl binding site. In *B* are shown the two cavities nearby the active site (marked *a* and *b*). Water molecules marked H located inside the cavities and around the active site are shown in *C*. Arg-215 is hydrogen-bonded to water molecules 20, 57, and 38. Polar residues are in *cyan*.

The Arg-215 and Met-211 residues were therefore changed to leucine and threonine, respectively, by means of the overlap extension method in PCR reactions (see "Experimental Procedures" for details). After confirming the mutations by DNA sequencing, the variant plasmids, together with the wild type as control, were transformed into *E. coli* BL21(DE3) cells, which were cultured in a small scale (100 ml) in LB-rich medium and induced with 0.1 mM IPTG for 3 h at a cell density corresponding to an optical density of 1 $A_{600\ nm}$. The harvested cells were disrupted with a French pressure cell, and after ultracentrifugation the clear lysate was taken as the crude extract. A preliminary screen for desired phenotypes was performed by assaying the crude extracts partially purified by thermo-precipitation of the *E. coli* protein at 70 °C for 15 min. An analysis on SDS-PAGE (not shown) suggested that the concentration of the two enzyme variants was comparable with that of the wild type. Equivalent amounts of partially purified extracts were assayed for esterase activity at 70 °C, with *p*NP esters as substrates, varying the acyl-chain length from 4 to 16 carbon atoms. After this preliminary analysis, the single mutant R215L was found to act better (about 2-fold increase in V_{max}) on esters with longer acyl chains (from 8 to 16 carbon atoms: data not shown), than both the wild type and single mutant M211T did. However, the mutant M211T displayed different characteristics from the wild type and was retained for further characterization (see below).

To further improve the phenotype obtained with R215L, we attempted a saturation mutagenesis approach. To this end, we took advantage of the availability of a filter assay for the rapid screening of mutants produced (see "Experimental Procedures"). The saturation mutagenesis was applied at position 211 to both the wild type and the R215L mutant. Clones were selected based on the activity ratio on β-naphthyl acetate and β-naphthyl laurate in the filter assay at room temperature, picked up and treated as described above. Variants with higher activity on β-naphthyl acetate were obtained, all derived from the wild type and displaying phenotypes similar to that of M211T (mutants M211S and M211V). A double-mutant M211S/R215L with a behavior slightly better than the single mutant was also obtained from R215L (data not shown).

Purification of EST2 variants and wild type and structural characterization by CD—The five variants and the wild type *est2* gene were transformed into *E. coli* BL21(DE3), cells were cultured at a large scale (2 liters) in LB medium, and the proteins were overexpressed and purified to homogeneity according to a described procedure (Ref. 8 and data not shown). The protein purity was checked by SDS-PAGE and found to be more than 98% as shown in Fig. 3. The protein yield and the chromatographic behavior for the variants was roughly comparable with that of the wild type, and, because the proteins were subjected to a thermo-precipitation step of purification, it was inferred that the introduced mutations did not significantly alter the three-dimensional structure of enzymes. In fact, it cannot be ruled out that the observed activity's increase was to be ascribed to destabilization in the structure (see "Discussion"). To ascertain the latter point, we compared the far (Fig. 4*A*) and near (Fig. 4*B*) UV spectra of the wild type and the five variants by CD measurements. Their thermal denaturation in the range 50–95 °C was monitored by the decrease in the CD signal at λ = 222 nm (Fig. 4*C*) and at λ = 290 nm (Fig. 4, *inset* of *panel B*). The far-UV spectra of variants were roughly superimposable to the wild type spectrum, thus suggesting no significant changes in the secondary structures. The near UV spectra (Fig. 4*B*) showed no differences in the range 280–320 nm, although there were some differences in the 260- to 280-nm region for mutant M211S (*red spectrum*), and for mutants R215L (*green spectrum*), and M211S/R215L (*magenta spectrum*). The thermal denaturation of wild type EST2 (Fig. 4*C*) monitored by changes in the α-helix content had a sigmoidal profile, with a temperature midpoint (see "Experimental Procedures") of 89.5 °C (*inset* of *panel C*) and without a complete denaturation at 95 °C, in agreement with previous results

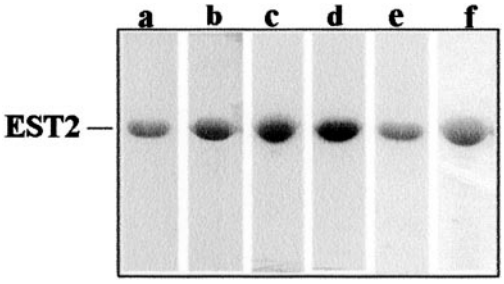

FIG. 3. **SDS-PAGE of purified wild type EST2 and mutants.** Amounts corresponding to 2.5 μg of wild type EST2 (*lane a*) and 5.0 μg of mutants R215L, M211S, R215L/M211S, M211T, and M211V (*lanes b*, *c*, *d*, and *e*, respectively) were loaded onto a 12.5% SDS-PAGE and stained by Coomassie Brilliant Blue G-250.

(9, 19). However, we did not observe any significant change in the thermostability of variants compared with the wild type (Fig. 4, *inset* of *panel C*) except for the M211T (*blue spectrum*), which displayed a temperature midpoint shifted of 1–2 °C toward lower temperatures. The same results were obtained by following the denaturation at $\lambda = 290$ nm (Fig. 4, *inset* of *panel B* and data not shown).

Kinetic Analysis of Wild Type EST2 and Variants at 70 °C—The kinetic constants of wild type and variants were measured against seven substrates and are reported in Table I. We preliminarily checked the pH dependence and the thermophilicity of all mutants and observed that these properties were unchanged (70 °C and pH 7.1) compared with the wild type (assays with substrate *p*NP-hexanoate; data not shown).

Enzyme kinetic constants were measured by using *p*NP esters of different acyl chain length. As reported previously (8), wild type EST2 showed maximal activity with *p*NP-hexanoate at 70 °C and pH 7.1.

Concerning the effect of mutations on k_{cat}, we observed that values for *p*NP-hexanoate slightly increased (for example, 30% with M211T) or decreased (33 and 54% with the double mutant and M211V, respectively). However, with other substrates the effect was considerably more impressive. In the case of mutant M211T, the k_{cat} for *p*NP-butanoate was 2.4-fold higher (5240 s^{-1}) than with wild type with the same substrate (2180 s^{-1}) and even increased (1.5-fold) when compared with wild type with its better substrate, *p*NP-hexanoate (3420 s^{-1}). A similar result was obtained with variants M211S and M211V, except that the latter had the same behavior as M211T with *p*NP-butanoate but not with *p*NP-hexanoate (1500 s^{-1}). In the case of mutant R215L, the activities with *p*NP-butanoate (3200 s^{-1}) and *p*NP-hexanoate (3660 s^{-1}) were comparable with the wild type, but activity was substantially higher on longer substrates. Notably, with C_{10}-C_{16} esters, activity almost doubled. The same result, an increase of ~2.5-fold in k_{cat}, was obtained with the double-mutant M211S/R215L on substrates C_{12}-C_{16}. It is worth noting that the described activity enhancements all occurred at 70 °C, the optimal temperature for the enzyme activity.

The analysis of the K_m values indicated that wild type affinity for *p*NP-hexanoate was 20-fold higher than the previously reported value (8). Because this value represents an assay mixture without solvents and detergents, we argued that the higher value found here was due to the presence of propan-2-ol in the assay mixture. The use of this solvent was essential to dissolve substrates and compare all enzymes in the same assay conditions. The observation that higher K_m values were obtained essentially only for substrates with acyl chains of four and six carbon atoms suggested a competitive effect toward the acyl chain. To ascertain this point, the EST2 activity was analyzed at three different concentrations of propan-2-ol and increasing concentrations of substrate *p*NP-hexanoate (Fig. 5). It turned out that the propan-2-ol behaves as a competitive inhibitor with an effect on K_m but not V_{max}, and the measured K_I was found to be 0.13 M. This experiment indicates that the measured K_m values shown in Table I are apparent values, thus they cannot be used to draw conclusions about the different substrate specificities and k_{cat} values, especially with shorter substrates. However, we confirmed that, for the M211T mutant, using *p*NP-butanoate as substrate, propan-2-ol still acts as a competitive inhibitor (data not shown) and measured a K_m value of 73 μM in its absence. This suggested a k_{cat}/K_m value of 42, which is about 1.4 times the value obtained for wild type in "water only" (8).

It is evident that the inhibitory effect of propan-2-ol is less severe, if at all, on longer substrates. In fact, the K_m measured for wild type with *p*NP-octanoate (28.5 μM) is lower than that measured previously in "water only" (43 μM (8)). If the above reasoning is correct, then the catalytic efficiency (k_{cat}/K_m) for acyl chains with greater than six carbon atoms represents the true enzyme preference for the substrate. As reported in Table I, higher values were obtained for R215L with *p*NP-decanoate and *p*NP-octanoate (2.3- and 1.8-fold the value of wild type with *p*NP-octanoate, respectively) and for double-mutant M211S/R215L with *p*NP-decanoate and *p*NP-dodecanoate (1.7- and 1.75-fold the value of wild type with *p*NP-octanoate, respectively). However, it is worth noting that the specificity constant of double-mutant M211S/R215L on substrate *p*NP-dodecanoate displayed a 6-fold higher value than the wild type with the same substrate.

EST2 Reaction Mechanism—To explain the above results, knowledge of the EST2 reaction mechanism was thought to be crucial. The general action mechanism of an esterase is shown in Fig. 6. Shortly, the enzyme (*E*) combines with ester substrate (S) to form the enzyme-substrate complex (*E*S), which is converted into the acyl-enzyme (*E*A) upon release of the alcohol. In the second part of the reaction, the attack of a nucleophile (water or alcohol) and the release of the acyl moiety, as such or as new ester, follow. If the alcohol release is the rate-limiting step, then k_{cat} corresponds to k_2. Alternatively, if the release of the acid/ester is slow, therefore $k_{cat} = k_3$. Because the mutations are located at the acyl binding pocket, it is predictable that they could affect the binding and/or the acid/ester release; in this circumstance, k_3 should be altered. However, we cannot dismiss the possibility of a long range effect resulting in an unusual binding of the *p*NP ester and an altered release of the alcohol (*e.g.* k_3 might also be affected). It was therefore vital to ascertain the action mechanism of both wild type EST2 and the mutants. The measurement of all the constants involved in the multistep reaction mechanism was outside the scope of the present paper, although it will be the subject of future work. However, one simple way to get a general idea about the reaction mechanism is to measure the *p*NP burst, which is supposed to occur when the enzyme is added to the reaction mixture before the onset of the catalytic reaction, provided the release of the acid/ester is slow compared with the release of the alcohol (32). Fig. 7 shows the results of such an experiment for the wild type and M211T with *p*NP-butanoate, for the wild type and R215L with *p*NP-decanoate, and for the wild type and the double-mutant M211S/R215L with *p*NP-dodecanoate. The *p*NP burst for the wild type was dependent on the substrate used. In fact, the immediate release of *p*NP increased proportionally to the concentration of the enzyme with *p*NP-butanoate, whereas with *p*NP-decanoate and *p*NP-dodecanoate, there was almost no change with the increase of enzyme concentration. This suggests that, with short substrates, the rate-limiting step is the acid/ester release ($k_2 \gg k_3$). Given that with

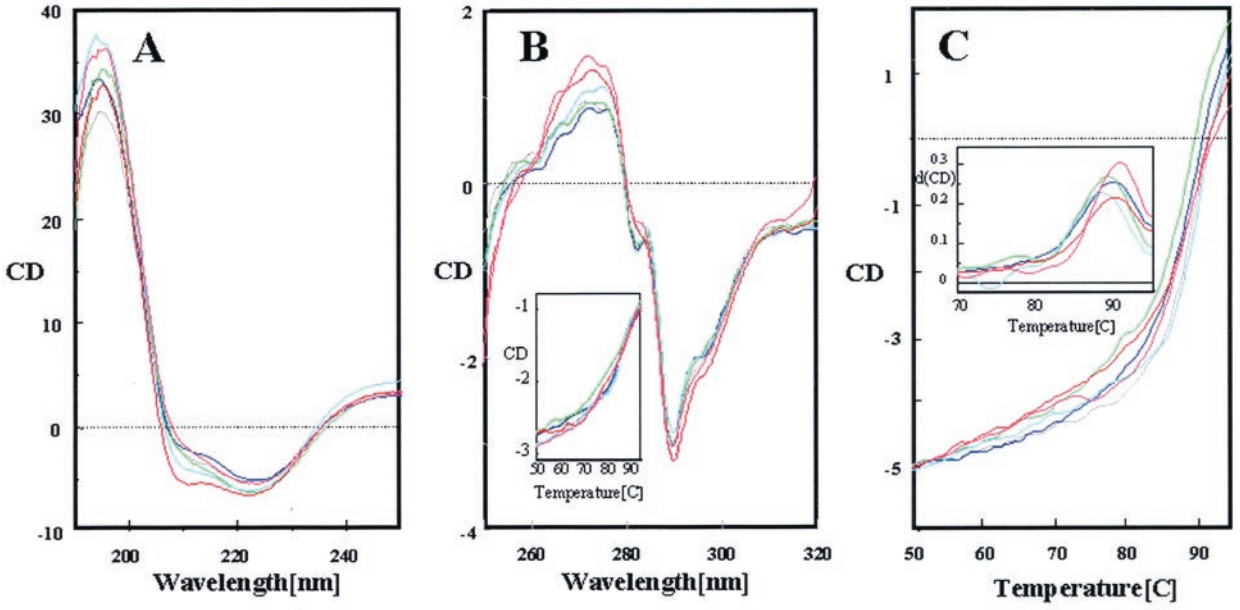

FIG. 4. **Structural characterization by CD of wild type EST2 and EST2 mutants.** *A*, far-UV CD measurements were performed in the range 250–190 nm, at 50 °C, and at a protein concentration of 0.10 mg/ml in 40 mM Na_2HPO_4/NaH_2PO_4 buffer. Spectra colored *gray*, *blue*, *green*, *cyan*, *red*, and *magenta* correspond to wild type, M211V, M211T, R215L, M211S, and R215L/M211S, respectively. *B*, CD measurements in the near-UV range were performed in the range 300–250 nm, at 40 °C, in 40 mM Na_2HPO_4/NaH_2PO_4 buffer, pH 7.1. The protein concentration was 0.3 mg/ml. The color code is as reported in *A*. In the *inset* the thermal denaturation curves of wild type EST2 and variants, which were monitored by following the ellipticity change at $\lambda = 290$ nm, in the conditions outlined in *A* and in the temperature range 50–95 °C, are reported. *C*, the thermal denaturation of wild type EST2 and variants was monitored in the range 50–95 °C by reading the ellipticity change at $\lambda = 222$ nm in the conditions outlined in *A*. The color code is as reported in *A*. In the *inset*, the first derivative transformations of spectra were reported.

TABLE I
Kinetic parameters of EST2 wild type and mutants

Data reported were mean of at least two experiments. The standard error was not higher than 5%.

Enzymes	Constants	Substrates						
		*p*NP-butanoate	*p*NP-hexanoate	*p*NP-octanoate	*p*NP-decanoate	*p*NP-dodecanoate	*p*NP-tetradecanoate	*p*NP-exadecanoate
Wild type	k_{cat} (s^{-1})	2180	3420	1960	950	390	105	21
	K_m (μM)	760	220	28	18	19	31	42
	k_{cat}/K_m ($s^{-1}\mu M^{-1}$)	3.0	15	69	52	21	3.0	0.5
R215L	k_{cat} (s^{-1})	3200	3660	3080	1670	705	232	35
	K_m (μM)	750	90	25	11	21	22	31
	k_{cat}/K_m ($s^{-1}\mu M^{-1}$)	4.0	41	126	158	34	10.5	1.1
M211S	k_{cat} (s^{-1})	4230	3890	1855	860	350	105	15.6
	K_m (μM)	1770	410	37	8.0	10	17	20.5
	k_{cat}/K_m ($s^{-1}\mu M^{-1}$)	2.4	9.0	50	107	35	6.0	0.8
M211S/R215L	k_{cat} (s^{-1})	2750	2300	1645	970	940	235	44
	K_m (μM)	1060	99	22	8.0	8.0	22	34
	k_{cat}/K_m ($s^{-1}\mu M^{-1}$)	3.0	23	75	116	120	11	1.3
M211T	k_{cat} (s^{-1})	5240 (3040)[a]	4440	1740	626	110	40	8.3
	K_m (μM)	1860 (73)	510	100	19	7.0	20	23
	k_{cat}/K_m ($s^{-1}\mu M^{-1}$)	3.0 (42)	9.0	17	33	16	2.0	0.4
M211V	k_{cat} (s^{-1})	4000	1500	1376	465	112	27	7
	K_m (μM)	1270	210	60	21	15	19	26
	k_{cat}/K_m ($s^{-1}\mu M^{-1}$)	3.0	7.0	23	22	7.0	1.4	0.3

[a] Numbers in parentheses refer to assays without propan-2-ol.

M211T and *p*NP-butanoate we get the same result as that obtained with the wild type (same slope), we concluded that the mechanism was unchanged. Therefore, the higher turnover number of the mutant can be explained by an increase in the rate of the acid/ester release ($k_3 = k_{cat}$), but this value should remain very low with respect to the constant leading to the alcohol release (k_2). The opposite scenario was observed with substrate *p*NP-dodecanoate. The absence of a *p*NP burst with the wild type and double-mutant M211S/R215L indicated that the reaction mechanism, in this case, was limited by the alcohol release. It is possible to imagine that the longer acyl chain in some way constrains the *p*NP moiety of the ester in a different binding mode that in turn results in a severe reduction in alcohol release. Again in the mutant, the turnover number increase should be ascribed to an increase in $k_2 = k_{cat}$, and, as in the case of the short substrate, we should consider a high difference in the values of the constants ($k_3 \gg k_2$).

The wild type behaves in the same way with substrate *p*NP-decanoate. The mechanism is still governed by the alcohol release, therefore $k_2 = k_{cat} \ll k_3$. Surprisingly, the result was different with the mutant R215L. It seems that, in this case, a switch occurs from the alcohol-controlled to the acid/ester-controlled reaction mechanism. In other words, the rate of alcohol release increases so that the mechanism becomes controlled by the acid/ester release. We measured an *p*NP burst, but the curve progression was not as steep as in the case of wild type and M211T with *p*NP-butanoate, thus suggesting a lower difference between k_2^* and k_3^*, with $k_3^* = k_{cat} < k_2^*$ (the aster-

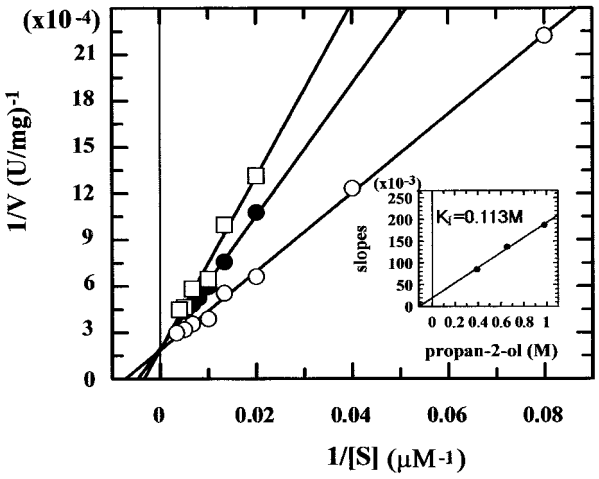

FIG. 5. **Propan-2-ol competitive inhibition of wild type EST2.** Shown is the Lineweaver-Burk plot of EST2 activity measured over the concentration range 12.5–300 μM of *p*NP-hexanoate in the presence of 0.39 M (○), 0.65 M (●), and 0.98 M (□), at 70 °C. In the *inset*, the slope of each line is replotted against the respective inhibitor concentration.

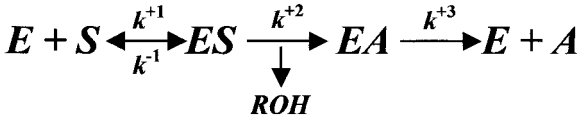

FIG. 6. **General mechanism of catalytic esterase activity.**

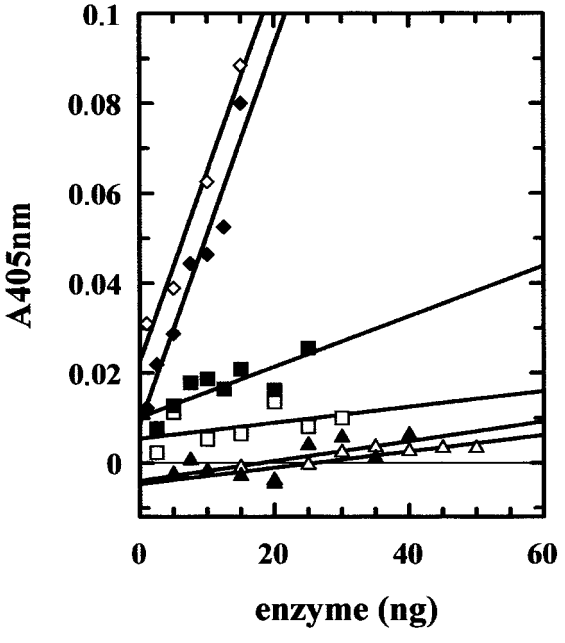

FIG. 7. **Instantaneous bursts of *p*NP measured after addition of wild type, M211T, R215L, or M211S/R215L enzymes to the assay mixture.** Shown are the readings at 405 nm and at time zero of assay mixtures containing *p*NP-butanoate, *p*NP-decanoate, or *p*NP-dodecanoate after the addition of indicated amounts of, respectively, wild type EST2 (◇) or M211T (◆); wild type EST2 (□) or R215L (■); and wild type EST2 (△) or the double mutant M211S/R215L (▲). Data were corrected for the *p*NP release due to the onset of the catalytic activity during the 4 s required to mix the enzyme with substrates and to read absorption.

isks refer to the changed mechanism). Obviously, in the latter case the situation should be $k_3^* > k_2$ to account for the higher activity of the mutant.

DISCUSSION

The accumulation of crystallographic data on thermostable and hyperthermostable enzymes (33, 34), together with statistic analyses (35–37) permitted by the rapid advancement of genome sequencing projects, has substantially improved our understanding of protein stability determinants. Academic curiosity is now tackling the issue of the relationship among stability/activity/flexibility of thermophilic proteins. The question is whether enzymes are finely tuned in terms of stability-lability so that this balance is crucial for function (38- 40). In other words, is it possible to engineer thermal stability in mesophilic enzymes without loosing catalytic activity or increase the activity, at times low, of thermophilic enzymes at low temperature, by preserving their thermal stability? The answer is not clear-cut. Directed evolution studies on psychrophilic and mesophilic enzymes (41–45) indicate that by accumulating several mutations it is possible to increase stability without sacrificing activity. The thermophilic thermolysin-like protease from *Bacillus stearothermophilus* was made more thermostable without any reduction in activity at 37 °C (46), and the activity of indoleglycerol-phosphate synthase from *Sulfolobus solfataricus* was improved at low temperature without loosing stability (47). The same result was reported for the ribonuclease H from *Thermus thermophilus* (48). However, in the β-glucosidase from *Pyrococcus furiosus* (49), it seems that stability and flexibility are highly optimized; in fact, mutants with improved activity at low temperature proved to be less stable. The same was found in the *Thermobifida fusca* exocellulase (50). Similar results were reported for several thermostable enzymes, which showed enhanced activity at low temperature in the presence of structural perturbants such as solvents or detergents, but at high temperature, they showed no activation and, on the contrary, destabilization (51, 52).

There are very few reports of mutations that increase activity of a thermophilic enzyme at its optimal temperature. Data reported in this paper indicate that, at least in this system, there is still room to improve activity at the optimal temperature of the enzyme, and this is not correlated with overall enzyme destabilization or changes in the temperature or pH dependence of activity.

The most striking result of this mutational approach to the study of the EST2 active site is the changes in substrate specificity afforded by single point mutations, as well as the increase in the turnover number with respect to the parental enzyme with some substrates and at high temperature.

Starting from an enzyme with preference for *p*NP-hexanoate, three mutants- M211S, M211T, and M211V- were obtained, all displaying their maximal activity on *p*NP-butanoate and probably, as demonstrated for M211T, similar k_{cat}/K_m for this substrate compared with the wild type. In addition, enzyme variants R215L, M211S, and the combination of the two, in the double-mutant M211S/R215L, showed increased activity and specificity constants on longer acyl chains compared with the wild type. The insertion of serine at position 211 was selected twice, as single and double mutation, from the screening procedure adopted, thus indicating a prominent role of the residue at this position for the specificity we screened for. The general increase in all variants of the turnover number compared with the parental enzyme was somewhat unexpected given that all assays were carried out at 70 °C, which is the optimal temperature for wild type activity, and a k_{cat} value of 3420 (6600 s^{-1} in "water only" (8)) is already a remarkable activity. For example, the acetylcholinesterase, a remote homologue of EST2 (9), has a k_{cat} value of 16,000 s^{-1}, and is considered one of the most active enzymes known (53).

Having found variants with higher catalytic activity at high

temperature, of which some had a change of substrate specificities, we were then faced with the problem of giving an interpretation to the above results. The sites for performing site-directed and saturation mutagenesis were chosen based on a careful analysis of the EST2 active site (Fig. 1*A*). Both the side chains of arginine 215 and methionine 211 were found to close the tunnel occupied by the HEPES molecule bound to the active-site serine. Because these residues are part of a α-helix (α7) and not of a loop, the k_{cat} increase cannot be interpreted as a change in loop flexibility due to the introduced mutations, as suggested for other enzymes in other works. For example, a change in the flexibility of a loop near the active site was demonstrated to be the motif of the activation at low temperature of an indoleglycerol-phosphate synthase mutant from *Sulfolobus solfataricus* (47). In addition, the change in a flexible loop was hypothesized to represent an enhancement of the exonuclease activity in a DNA polymerase mutant from *Thermococcus aggregans* (54).

The choice of positions for mutations insertion into EST2 was made based on the above-cited considerations on sequence comparison with lipases as well as the observed interactions of Arg-215 and Met-211 with the HEPES inhibitor. It is therefore predictable that the observed effects occurred due to an interference with the binding mechanism and/or the release of the acyl/ester moiety to/from the active site. Arg-215 was mutagenized in the hydrophobic and smaller residue leucine. The mutation of arginine into leucine could have an effect on the bond water, because the side chain of arginine is connected through hydrogen bonds to water molecules 20 and 57 (both placed inside cavity b), and by two hydrogen bonds with a second couple of water molecules (38 and 51) nearby. This interpretation also stems from the analysis of the near-UV CD data. The double-mutant M211S/R215L and the M211S mutant spectra deviate from the wild type spectrum, especially in the 260- to 280-nm range. A minor effect was observed for R215L. Excluding the contribution of disulfide bonds that are absent in EST2, in the above-cited region the bands of phenylalanines, tyrosines, and tryptophans overlap. If conformational effects are related only to the active site as suggested by structural and kinetic data, it should be observed that Trp-85, Tyr-188, and Phe-214 participate in forming cavity b (Fig. 2*B*). In particular, with its OH group and backbone O, Tyr-188 forms two hydrogen bonds with water molecules 38 and 51, respectively. In addition, Trp-85 is located very close to Arg-215, whereas Met-211 is next to Phe-214. It is conceivable that mutations affecting the binding of water molecules could switch the lateral chains of these residues, and Tyr-188 in particular, to less symmetric environments (*e.g.* more rigid), thus resulting in the observed enhancement of the CD signal in the near UV.

The arrangement of buried cavities constellated with polar and charged residues bound to ordered water molecules found in EST2 is reminiscent of similar findings in a group of fungal lipases (55). Two hypotheses were made to explain the role of these unusual buried polar clusters. Some authors (56) have suggested they were involved in the catalytic activity to supply a pool of water molecules for the nucleophilic attack in the second stage of the hydrolytic reaction. Others (55) have speculated that these structural anomalies were related to the interfacial activation mechanism and in particular to the stabilization of the enzyme in the lipid-bound form. Given that EST2 acts primarily on substrates in solution and does not show any interfacial activation, the former hypothesis is likely to be the least appropriate to explain the presence of some buried cavities nearby the active site. The a cavity could better fulfill this role, because it is located more closely to the tetrahedral intermediate. However, the mutation does not negatively affect the catalytic activity, as shown here. Because the arginine is not conserved in the H group but is substituted by smaller residues, it is also unlikely that these water molecules are involved in the hydrolysis of the acyl-enzyme complex. Finally, a molecular modeling approach for the evaluation, by energy minimization in the absence of water, of the effect of the arginine substitution in leucine indicates (data not shown) a dramatic reduction in this cavity. Considering all of this, we hypothesize that this cavity has a role in the EST2 substrate specificity. In particular, through water displacement and filling of the cavity, it could allow for the binding of a number of different substrates. In fact, a common characteristic of carboxylesterases is their broad range of specificity. In the mutant, the reduction in size of this cavity and possibly of the number of bound-water molecules, together with the reduction in the side-chain length at position 215 and the increase in its hydrophobicity, could result in a better binding of esters with longer acyl chains. This hypothesis is supported by the decrease in the K_m values for substrates with longer acyl chains for the R215L mutant. The better binding at the acyl site can result, as hypothesized above, in a less constrained binding of the alcohol moiety at the alcohol-binding site, thus allowing a higher k_{cat} with respect to the wild type. To explain the higher activity of variants mutated at position 211 toward substrates with shorter acyl chains, the above-cited suggestion of a mechanism controlled by the acid/ester release, provided a plausible explanation. In actual fact, if the methionine has a steric hindrance *versus* the acid/ester release, then substitution with residues with shorter side chains could allow for a better release of the acid/ester and consequently for higher k_{cat} values. The K_m values again are lower than in the wild type starting from *p*NP-decanoate. In the double mutant, the latter effect is synergic with the reduced steric hindrance and the major local hydrophobicity allowed by the substitution of a charged residue with a hydrophobic one, providing an explanation for the higher specificity found with longer acyl chains starting from decanoate.

The results reported in this study provide experimental support to the idea that the activity of some enzymes must to be reduced at high temperature, to cope with the metabolism of the microorganisms (57) and that the modern approach of evolution in the "test tube" could allow for the production of such variants, which nature has selected against. This is also the first report on a mutational analysis of the active site of a thermophilic esterase and a member of the HSL family, which could represent a comparative basis for the study of the medically important human homologous HSL (58). By single mutations at the active site, we were able to simultaneously change specificity and improve activity of a thermophilic esterase without changing its thermophily and thermostability. The results obtained are intriguing from both an academic and biotechnological point of view.

Acknowledgment—We thank Dr. G. Adamo for preparation of plasmid pT7-SCII-AG.

REFERENCES

1. Krejci, E., Duval, N., Chatonnet, A., Vincens, P., and Maussolìe, J. (1991) *Proc. Natl. Acad. Sci. U. S. A.* **88,** 6647–6651
2. Hemilä, H., Koivula, T. T., and Palva, I. (1994) *Biochim. Biophys. Acta* **1210,** 249–253
3. Langin, D., Laurell, H., Stenson-Holst, L., Belfrage, P., and Holm, C. (1993) *Proc. Natl. Acad. Sci. U. S. A.* **90,** 4897–4901
4. Klenk, H. P., Clayton, R. A., Tomb, J. F., White, O., Nelson, K. E., Ketchum, K. A., Dodson, R. J., Gwinn, M., Hickey, E. K., Peterson, J. D., Richardson, D. L., Kerlavage, A. R., Graham, D. E., Kyrpides, N. C., Fleischmann, R. D., Quackenbush, J., Lee, N. H., Sutton, G. G., Gill, S., Kirkness, E. F., Dougherty, B. A., McKenney, K., Adams, M. D., Loftus, B., Venter, J. C., *et al.* (1997) Nature **390,** 364–370
5. Manco, G., Adinolfi, E., Pisani, F. M., Carratore, V., and Rossi, M. (1997) *Prot.*

Pept. Lett. **4,** 375–382
6. Manco, G., Giosue', E., D'Auria, S., Herman, P., Carrea, G., and Rossi, M. (2000) *Arch. Biochem. Biophys.* **373,** 182–192
7. Holm, C., Kirchgessner, T. G., Svenson, K. L., Fredrikson, G., Nilsson, S., Miller C. G., Shively, J. E., Heinzmann, C., Sparkes, R. S., Mohandas, T., Lusis, A. J., Belfrage, P., and Schotz, M. C. (1988) *Science* **241,** 1503–1506
8. Manco, G. Adinolfi, E., Pisani, F. M., Ottolina, G., Carrea, G., and Rossi, M. (1998a) *Biochem. J.* **332,** 203–212
9. Manco, G., Febbraio, F., Adinolfi, E., and Rossi, M. (1999) *Protein Sci.* **8,** 1789–1796
10. Manco, G., Febbraio, F., and Rossi, M. (1998b) *Prog. Bio/Technol.* **15,** 325–330
11. Manco, G., Camardella, L., Febbraio, F., Adamo, G., Carratore, V., and Rossi, M. (2000) *Protein Eng.* **13,** 197–200
12. Wei, Y., Contreras, J. A., Sheffield, P., Osterlund, T., Derewenda, U., Kneusel, R. E., Matern, U., Holm, C., and Derewenda, Z. S. (1999) *Nat. Struct. Biol.* **6,** 340–345
13. De Simone, G., Galdiero, S., Manco, G., Lang, D., Rossi, M., and Pedone, C. (2000) *J. Mol. Biol.* **303,** 761–771
14. Ollis, D. L., Cheah, E., Cygler, M., Dijkstra, B., Frolow, F., Franken, S. M., Harel, M., Remington, S. J., Silman, I., Schrag, J., Sussman, J. L., Verschueren, K. H. G., and Goldman, A. (1992) *Protein Eng.* **5,** 197–211
15. Derewenda, Z. S. (1994) *Adv. Protein Chem.* **45,** 1–52
16. Nardini, M., and Dijkstra, B. W. (1999) *Curr. Opin. Struct. Biol.* **9,** 732–737
17. Heikinheimo, P., Goldman, A., Jeffries, C., and Ollis, D. L. (1999) *Structure Fold. Des.* **7,** R141–R146
18. Cousin, X., Hotelier, T., Giles, K., Toutant, J. P., and Chatonnet, A. (1998) *Nucleic Acids Res.* **26,** 226–228
19. D'Auria, S., Herman, P., Lakowicz, J. R., Bertoli, E., Tanfani, F., Rossi, M., and Manco G. (2000) *Proteins* **38,** 351–360
20. D'Auria, S., Herman, P., Lakowicz, J. R., Tanfani, F., Bertoli, E., Manco, G., and Rossi, M. (2000) *Proteins* **40,** 473–481
21. Desnuelle, P. (1972) in *The Enzymes* (Boyer, P. D., ed) pp. 575–616, pp. 194–288, Academic Press, New York
22. Brockerhoff, H., and Jensen, R. G. (1974) in *Lipolytic Enzymes*, pp. 194–288, Academic Press, New York
23. Niehaus, F., Bertoldo, C., Kahler, M., and Antranikian, G. (1999) *Appl. Microbiol. Biotechnol.* **51,** 711–729
24. Kim, M. H., Kim, H. K., Lee, J. K., Park, S. Y., and Oh, T. K. (2000) *Biosci. Biotechnol. Biochem.* **64,** 280–286
25. Cho, A. R., Yoo, S. K., and Kim, E. J. (2000) *FEMS Microbiol. Lett.* **186,** 235–238
26. Schmidt-Dannert, C., Rua, M. L., and Schmid, R. D. (1997) *Methods Enzymol.* **284,** 194–220
27. Brown, W. C., and Campbell, J. L. (1993) *Gene* **127,** 99–103
28. Sambrook, J., Fritsch, E. F., and Maniatis, T. (1989) *Molecular Cloning: A Laboratory Manual*, 2nd Ed., Cold Spring Harbor Laboratory, Cold Spring Harbor, NY
29. Ho, S. N., Hunt, D. H., Horton, R. M., Pullen, J. K., and Pease, L. R. (1989) *Gene* **77,** 51–59
30. Leatherbarrow, R. J. (1992) *Grafit Version 3.0*, Erithacus Softwere Ltd., Staines, UK
31. Laemmli, U. K. (1970) *Nature* **227,** 680–685
32. Hartley, B. S., and Kilby, B. A. (1952) *Biochem. J.* **60,** 672
33. Szilàgyi, A., and Zàvodszky, P. (2000) *Structure* **8,** 493–504
34. Cambillau, C., and Claverie, J. M. (2000) *J. Biol. Chem.* **275,** 32383–32386
35. McDonald, J. H., Grasso, A. M., and Rejto, L. K. (1999) *Mol. Biol. Evol.* **16,** 1785–1790
36. Haney, P. J., Badger, J. H., Buldak, G. L., Reich, C. I., Woese, C. R., and Olsen, G. J. (1999) *Proc. Natl. Acad. Sci. U. S. A.* **96,** 3578–3583
37. Thompson, M. J., and Eisenberg, D. (1999) *J. Mol. Biol.* **290,** 595–604
38. Arnold, F. H. (1999) *Proc. Natl. Acad. Sci. U. S. A.* **95,** 2035
39. Závodszky, P., Kardos, J., Svingor, Á., and Petsko G. A. (1998) *Proc. Natl. Acad. Sci. U. S. A.* **95,** 7406–7411
40. Somero, G. N. (1995) *Annu. Rev. Physiol.* **57,** 43–68
41. Giver, L., Gershenson, A., Freskgard, P. O., Arnold, F. H. (1998) *Proc. Natl. Acad. Sci. U. S. A.* **95,** 12809–12813
42. Spiller, B., Gershenson, A., Arnold, F. H., and Stevens, R. C. (1999) *Proc. Natl. Acad. Sci. U. S. A.* **96,** 12305–12310
43. Gershenson, A., Schauerte, J. A., Giver, L., and Arnold, F. H. (2000) *Biochemistry* **39,** 4658–4665
44. Miyazaki, K., Wintrode, P. L., Grayling, R. A., Rubingh, D. N., and Arnold, F. H. (2000) *J. Mol. Biol.* **297,** 1015–1026
45. Wintrode, P. L., Miyazaki, K., and Arnold, F. H. (2000) *J. Biol. Chem.* **275,** 31635–31640
46. Van Den Burg, B., Vriend, G., Veltman, O. R., Venema, G., and Eijsink, V. G. H. (1998) *Proc. Natl. Acad. Sci. U. S. A.* **5,** 2056–2060
47. Merz, A., Yee, M. C., Szadkowski, H., Pappenberger, G., Crateri, A., Stemmer, W. P., Yanofsky, C., and Kirschner, K. (2000) *Biochemistry* **39,** 880–889
48. Hirano, N., Haruki, M., Morikawa, M., and Kanaya, S. (2000) *Biochemistry* **39,** 13285–13294
49. Lebbink, J. H., Kaper, T., Bron, P., van der Oost, J., and de Vos, W. M. (2000) *Biochemistry* **39,** 3656–3665
50. Zhang, S., Barr, B. K., and Wilson, D. B. (2000) *Eur. J. Biochem.* **267,** 244–252
51. Guagliardi, A., Manco, G., Rossi, M., and Bartolucci, S. (1989) *Eur. J. Biochem.* **183,** 25–30
52. D'Auria, S., Barone, R., Rossi, M., Nucci, R., Barone, G., Fessas, D., Bertoli, E., and Tanfani, F. (1997) *Biochem. J.* **323,** 833–840
53. Hasan, F. B., Cohen, S. G., and Cohen, J. B. (1980) *J. Biol. Chem.* **255,** 3898–3904
54. Bohlke, K., Pisani, F. M., Vorgias, C. E., Frey, B., Sobek, H., Rossi, M., and Antranikian, G. (2000) *Nucleic Acids Res.* **28,** 3910–3917
55. Derewenda, U., Swenson, L., Green, R., Wei, Y., Dodson, G. G., Yamaguchi, S., Haas, M. J., and Derewenda, Z. S. (1994) *Nat. Struct. Biol.* **1,** 36–47
56. Schrag, J. D., Li, Y. G., Wu, S., and Cygler, M. (1991) *Nature* **351,** 761–764
57. Somero, G. N. (1983) *Comp. Biochem. Physiol. A.* **76,** 621–33
58. Georis, J., de Lemos Esteves, F., Lamotte-Brasseur, J., Bougnet, V., Devreese, B., Giannotta, F., Granier, B., and Frere, J. M. (2000) *Protein Sci.* **9,** 466–475

Residues at the Active Site of the Esterase 2 from *Alicyclobacillus acidocaldarius* Involved in Substrate Specificity and Catalytic Activity at High Temperature

Giuseppe Manco, Luigi Mandrich and Mosè Rossi

J. Biol. Chem. 2001, 276:37482-37490.
doi: 10.1074/jbc.M103017200 originally published online July 10, 2001
